Journal of Alloys and Compounds 509 (2011) 10110–10114

Contents lists available at ScienceDirect

Journal of Alloys and Compounds

journal homepage: www.elsevier.com/locate/jallcom

Characterization of chromium thin films by sputter deposition

Sea-Fue Wang[a,*], Hsui-Chi Lin[a], Hui-Yun Bor[b], Yi-Lung Tsai[b], Chao-Nan Wei[b]

[a] Department of Materials and Mineral Resources Engineering, National Taipei University of Technology, Taipei 106, Taiwan
[b] Materials & Electro-Optics Research Division, Chung-Shan Institute of Science & Technology,Taiwan, ROC

ARTICLE INFO

Article history:
Received 22 September 2010
Received in revised form 2 August 2011
Accepted 10 August 2011
Available online 19 August 2011

Keywords:
Chromium thin films
Optical properties
Sputtering

ABSTRACT

In this study, a systematic investigation on the deposition of Cr–CrO_x bi-layer film was performed by magnetron DC sputtering. The X-ray photoelectron spectrometer (XPS) examining the bare Cr film showed that the peaks of Cr $2P_{3/2}$ and Cr $2P_{1/2}$ appeared in the Cr thin film associated with the presence of a 12 nm oxide layer. The transmission was reduced to zero as the Cr film exceeded 100 nm in thickness. The reflection saturated at a value of ≈55% when the thickness of the Cr film reached 30 nm. The optical density exceeded 3.50 with a Cr film thickness over 150 nm. In order to reduce the reflection of the film to a level of ≤4%, a Cr–CrO_x bi-layer thin film was prepared. Overall, a Cr–CrO_x bi-layer film with the Cr layer 130 nm and the CrO_x layer 40 nm in thickness reported a transmission of zero, a reflection of 3.82% and an optical density of 4.04, all meeting the requirements of anti-reflection black matrix (BM) for display applications.

1. Introduction

Both a pioneer and a mainstay in the flat panel display (FPD) market, liquid crystal display (LCD) has been confronting ever-intensifying competition from challengers like plasma display, field emission display (FED), and organic light emitting diode (OLED). LCD makers are therefore working with great vitality to reduce manufacturing cost and enhance productivity. A LCD panel consists of two glass substrates: the CF (color filter) substrate and the driving substrate. Color filter serves as a core component of LCD, accounting for 30% of the entire cost of a LCD module. It integrates layers of the three primary colors with a black matrix (BM) to help the panel mix a variety of colors. Color filter as an indispensable LCD component affects not only the color characteristics of the display panel but also the contrast ratio, luminance, and reflections on its surface properties. The quality of color filter plays a decisive role influencing the overall performance of LCD [1–3]. Black matrix, on the other hand, comprises a functional film used to improve the contrast ratio of flat-panel displays due to the light-shading function for driving electrodes in thin film transistors and preventing the inappropriate mixing of colorants in color filters [4]. Materials used currently in black matrix include Cr, its oxide/nitride combinations [5,6], and black carbon resin [7,8]. The characteristics of Chromic BM and anti-reflection chromic BM are summarized in Table 1 [9–12].

After the use of hexavalent chromium in chromium electroplating was found to induce cancer [13], alternative deposition techniques have been developed, such as spray [14], ion plating [15], sputtering [16], ion implantation [17], and trivalent chromium plating [18]. Though few study have been reported in the literature regarding the Cr based [19] or its oxide/nitride multilayer for use in BM, such as CrO_x–Cr for high-resolution color cathode-ray tube application [16] and oxide–nitride combination layers for color filter application [19], knowledge regarding the processing/microstructure/property relations remains rare in open literature [16,19]. In this paper, a systematic study on the preparation of Cr–CrO_x bi-layer films was performed by magnetron DC sputtering. Processing parameters of sputtering power and sputtering time, and the effects of film thickness on the optical properties of the Cr–CrO_x bi-layer films were investigated and discussed through X-ray diffractometer (XRD), XPS (Omicron Multiprobe Compact) and optical characterizations.

2. Experimental

Cr films were deposited on glass substrates (EAGLE^{2000TM}, Corning Incorporated) by D.C. magnetron sputtering (Kao Duen Technology Corporation, Taiwan) of a high purity chromium target (99.99%) in a chamber with a base pressure higher than 7×10^{-6} Torr. Prior to the deposition, glass EAGLE^{2000TM} with a dimension of 30 mm × 30 mm × 0.7 mm was cleaned for 15 min in an ultrasonic cleaner with a solution consisting of acetone, methyl-alcohol and DI water and dried by a nitrogen blower. The chromium target was characterized and reported a BCC structure with a density of 7.19 g/cm^3 (correspond to 99% of theoretical density) and an average grain size of 108 μm. Films were sputtered onto glass substrates without being heated, resulting in a deposition temperature of ~80 °C (measured using

* Corresponding author at: National Taipei University of Technology, Department of Materials and Mineral Resources Engineering 1, Sec. 3, Chung-Hsiao E. Rd., Taipei 106, Taiwan. Tel.: +886 2 0919 328 953; fax: +886 2 8773 2608.
E-mail address: sfwang@ntut.edu.tw (S.-F. Wang).

0925-8388/$ – see front matter © 2011 Elsevier B.V. All rights reserved.
doi:10.1016/j.jallcom.2011.08.052

Table 1
Characteristics of chromic BM and anti-reflection chromic BM.

Categories	Chromic BM	Anti-reflection chromic BM
Material	Cr	CrO_x–Cr
Method of pattern formation	Etching	Etching
Thickness of thin film	0.13	0.17
O.D.	>3.5	>4
Reflection	50–60%	≤4%
Line accuracy rate	±0.2 μm	±0.2 μm

thermocouple under the glass substrate). D.C. power for the sputtering varied from 10 W to 100 W, and the working gas was maintained at 5×10^{-3} Torr for sputtering the films. Atmosphere effects including pressure and composition on the film characteristics were studied and optimized. Pure argon was used to deposit the Cr films. Different ratios of the argon and oxygen mixture were pioneered for depositing CrO_x films and the ratio of 1:1 was chosen in this study after examining the efficiency of the CrO_x formation. The argon and oxygen gases used in deposition have a purity of at least 99.99%. Prior to deposition, the target was sputter-cleaned for at least 10 h.

Crystallographic evolution of the films was examined and crystallized phases identified by a thin film XRD (Rigaku D/max-B) with monochromatic Cu Kα radiation. Microstructural analyses were performed by a field emission scanning electron microscope (FESEM, HITACHI S-4700). The film thickness of the films was measured using FESEM and thereafter the deposition rates were determined. Composition profiles and chemical states of the elements were analyzed using a XPS. The optical properties were measured by UV–vis spectrophotometers (LAMBDA 900).

3. Results and discussion

3.1. Characteristics of Cr thin film

Cr thin films deposited at various DC powers were examined by XRD, and the results are shown in Fig. 1. The film was amorphous when deposited at a sputtering power of 10 W while well crystalline Cr thin film characterized with Cr {1 1 0} peak emerged in the XRD patterns at the sputtering powers of 30, 50, 80, and 100 W. The intensities of the {1 1 0} peak were found to slightly depend on the sputtering power. The peak position shifted to a small angle as the sputtering power above 50 W due to residual stress. Fig. 2 shows the cross-section SEM micrograph of Cr thin films deposited at the sputtering powers of 100 and 50 W for 10 min. As indicated, films with a smooth surface and columnar grains perpendicular to the glass substrate were obtained in this study, except the amorphous film obtained at the sputtering powder of 10 W. The porosity on the film surface and the roughness of the films seem to increases with sputtering power. The deposition rates of the Cr thin films at the

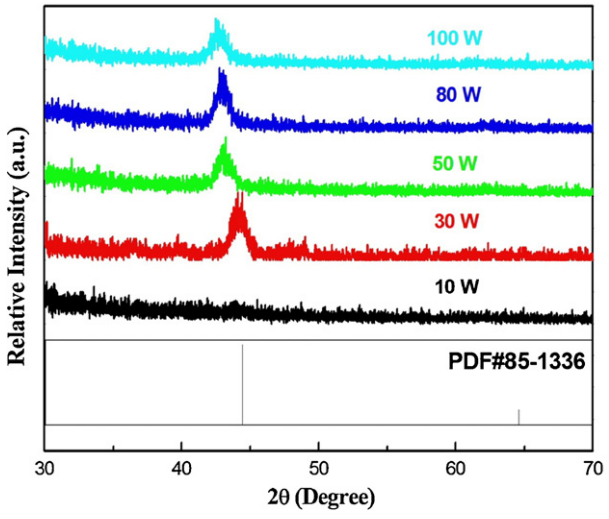

Fig. 1. X-ray diffraction patterns of Cr thin film deposited at sputtering powers of 10, 30, 50, 80, and 100 W.

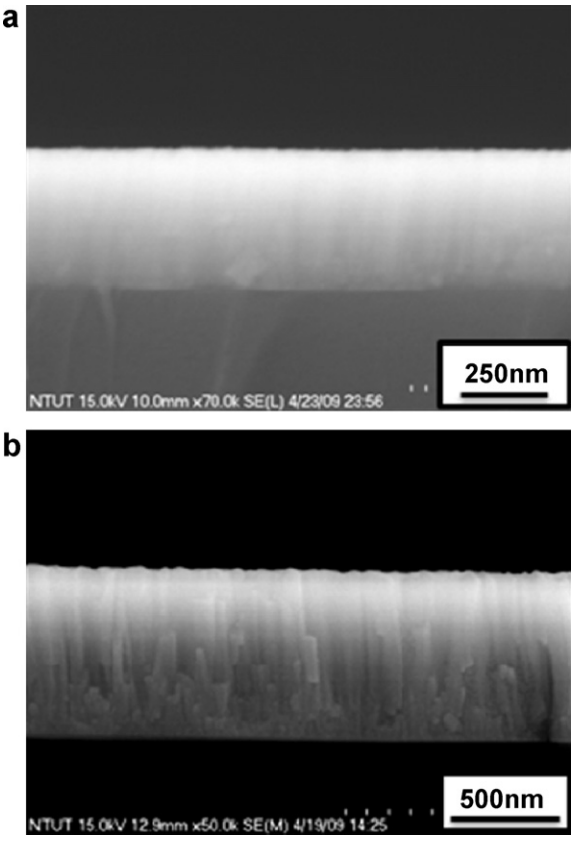

Fig. 2. Cross-section SEM micrograph of Cr thin films deposited at sputtering powers of (a) 50 W and (b) 100 W for 10 min.

sputtering powers of 10, 30, 50, 80, and 100 W were calculated to be 9, 35, 45, 73, and 88 nm/min, respectively.

Fig. 3(a) and (b) shows the XPS spectra of the Cr thin film deposited at a sputtering power of 100 W before and after sputter-etching. The XPS spectra were excited by monochromatized Al Kα radiation ($h\nu$ = 1486.6 eV). During XPS measurements, the specimens were first sputtered with Ar ions to remove surface contamination or surface oxidation. Fig. 4 presents the elemental depth profiles of the Cr thin film obtained from the XPS analysis for different etching time. Curve-fitted by the least-squares method using the Gaussian–Lorentzian envelope (red line in the figure), the Cr thin films before sputter-etching was observed to be characterized with four peaks in the XPS spectra [Fig. 3(a)], which correspond to four different chemical species including metallic chromium (574.3 and 284.2 eV), Cr_2O_3 (586.3 eV), and oxidic or hydroxydic Cr (Cr_2O_3, $Cr(OH)_3$, CrO(OH), 276.3–578.3 eV) [20–22].(For interpretation of the references to color in this text, the reader is referred to the web version of the article.) While only the peaks of Cr $2P_{3/2}$ and Cr $2P_{1/2}$ appeared in the Cr film after sputter-etching, it is evident from the XPS analysis that a thin chromium-oxide layer is present on the surface of the Cr thin film due to oxygen absorption as the Cr thin film was exposed to atmosphere. The oxide layer stabilized at a thickness of ≈12 nm based on the results shown in Fig. 4. Thanks to its dense and inert nature, the chromium-oxide layer on the surface of the Cr thin film acted as a protection layer against further oxidation of Cr.

A sputtering power of 30 W was then selected for the depositions of the Cr thin film to characterize its optical properties. Fig. 5 shows the optical transmittance, reflective spectra and optical density spectra of the Cr thin films with thickness range of 0–500 nm, measured at a light wavelength of 550 nm. The optical properties of Cr films were immediately measured after the films being

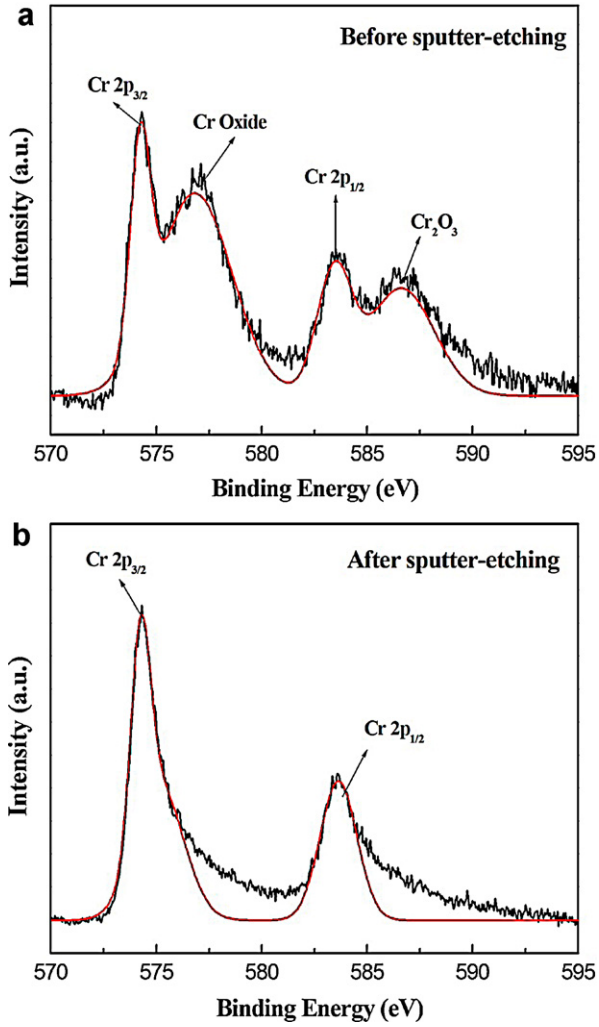

Fig. 3. XPS spectra of the Cr thin film deposited at sputtering power of 100 W (a) before and (b) after sputter-etching.

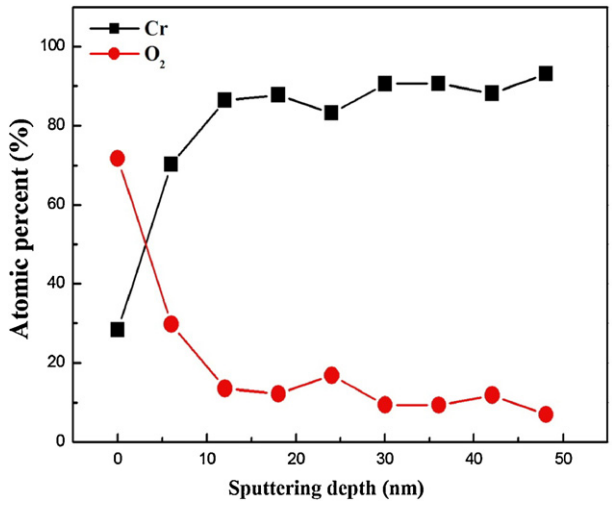

Fig. 4. Elemental depth profiles of Cr thin film obtained from XPS analysis for different etching time.

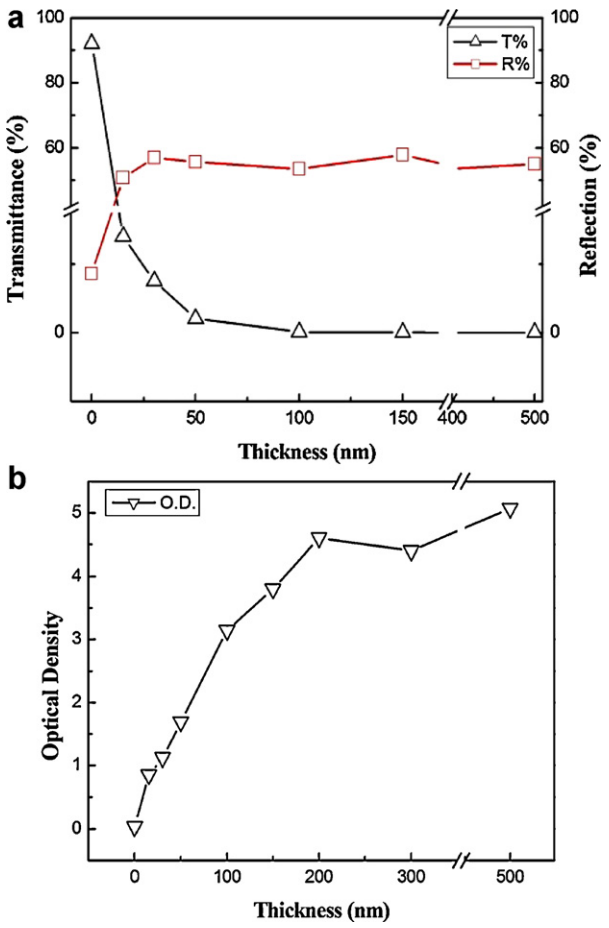

Fig. 5. (a) Optical transmittance and reflection spectra and (b) optical density spectra of Cr thin films vs. film thickness, deposited at a sputtering power of 30 W and measured at a light wavelength of 550 nm.

deposited and the samples were consequently stored in the vacuumed desiccators. The native layer with limited thickness seemed not to place a significant effect on the optical properties. The bare glass substrate reported a transmission of 92% that plummeted to 14.05% when, on top of the substrate, a 15 nm Cr thin film was deposited and exhibited metallic luster. The transmission dropped further to 2.05% as the film thickness increased to 50 nm and sank slowly to zero when the thickness of the Cr thin film exceeded 100 nm [Fig. 5(a)]. The reflection of the Cr thin film increased with its thickness up to 30 nm. Hitting 50% when the film thickness read a relatively thin 15 nm, the reflection saturated at a value of ≈55% as the thickness of the Cr thin film reached 30 nm and then stayed virtually constant in spite of further increase in film thickness. The reflection of chromium metal is lower than those of other metals, making it compatible with the use as a shading layer. The optical density (O.D.) can be calculated according to the Beer–Lambert Law of O.D. = $-\ln(1/T)$, in which T corresponds to the transmittance of the films [4], and the results are shown in Fig. 5(b). The optical density registered an obvious increase with film thickness, ranging from 0.85 to 5.07 as the film thickness rose from 15 nm to 500 nm. The value reached 3.5 when the thickness of the Cr thin film approached 150 nm, meeting the criteria for shading layer specification (Table 1).

3.2. Characteristics of the Cr–CrO_x bi-layer films

In order to further reduce the reflection of the Cr thin film, a Cr–CrO_x bi-layer thin film was fabricated for application in

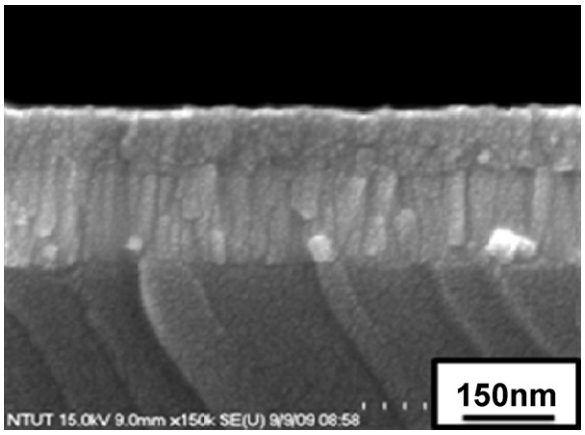

Fig. 6. Cross-section SEM micrograph of Cr–CrO_x bi-layer film (Cr thin film deposited at a sputtering power of 30 W and under pure Ar atmosphere; and CrO_x at a sputtering power of 100 W and under a mixture of argon and oxygen (1:1)).

anti-reflection BM. Deposition of Cr thin film was performed at a sputtering power of 30 W and under pure Ar atmosphere. The nominal thickness of the Cr film is set at 130 nm. Chromium oxide in various thicknesses ranging from 20 to 100 nm was deposited on the top of the Cr thin film at a sputtering power of 100 W and under an atmosphere of Ar and O_2 mixture (1:1). The deposition rate of the CrO_x was determined to be 21 nm/min. Fig. 6 shows the typical cross-section SEM micrograph of the Cr–CrO_x bi-layer film, which indicates a relatively smooth and uniform interface and surface. As indicated in the SEM micrograph, Cr films with columnar grains perpendicular to the glass substrate and granular CrO_x layer adjacent to the Cr film were obtained in this study. The surface roughness of the bilayer films ranging from 1.47 nm to 2.67 nm. The oxide layer deposited served as a barrier layer to avoid additional oxidation, which allowed us to modify the optical properties by monitoring the thicknesses of the Cr and CrO_x films.

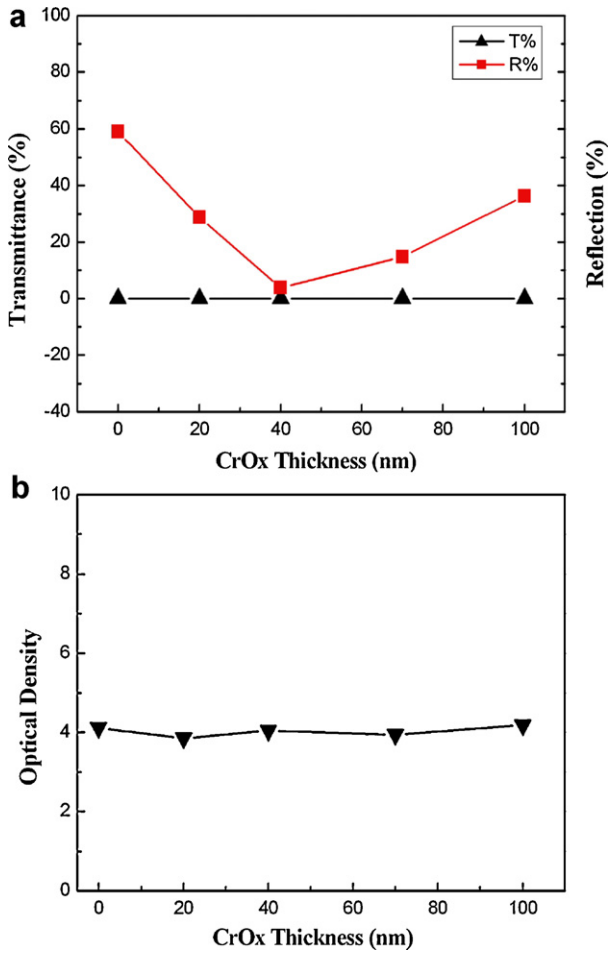

Fig. 7. (a) Optical transmittance and reflection and (b) optical density as function of CrO_x thickness in Cr–CrO_x bi-layer thin film (thickness of Cr thin film ≈130 nm).

Fig. 7(a) and (b) shows respectively the optical transmittance, reflection and optical density of the Cr–CrO_x bi-layer thin film as a function of CrO_x thickness with the Cr thin film reporting a thickness of 130 nm. As indicated by previous results, the transmission of the single Cr thin film read zero as its thickness approached 100 nm. It was thus expected that the Cr–CrO_x thin film was not light transparent [Fig. 7(a)]. The reflection of the Cr–CrO_x thin film appeared to be strongly dependent on the thickness of the deposited CrO_x layer, decreasing from the bare Cr film with a 59% transmission to the Cr–CrO_x bi-layer film with 40 nm of CrO_x having a 3.82% transmission; the transmission then turned around and increased with the thickness of the CrO_x film. This is due to the well known effect of destructive interference, which is dependent on the wavelength of light. If the thickness of CrO_x is equal to a quarter-wavelength of the incident light (550 nm) and if the light strikes the film at normal incidence, the reflected waves will be completely out of phase and will destructively interfere. The optical density of the Cr–CrO_x bi-layer film read ≈4 [Fig. 7(b)], regardless to the thickness of the CrO_x layer. On the whole, a Cr–CrO_x bi-layer film with the Cr film 130 nm and the CrO_x film 40 nm in thickness reported a transmission of zero, a reflection of 3.82% and an optical density of 4.04, all meeting the requirements of anti-reflection chromic BM.

4. Summary

In this study, a systematic investigation on the preparation of Cr and CrO_x bi-layer film was performed by magnetron DC sputtering. The processing parameters and the effects of film thickness on the optical properties of the Cr–CrO_x bi-layer films were examined and discussed through XRD, XPS and optical characterization. XPS results confirmed the presence of a 12 nm oxide layer in the bare Cr-film due to absorption in the atmosphere. A Cr–CrO_x bi-layer film with the Cr film 130 nm and the CrO_x film 40 nm in thickness reported a transmission of zero, a reflection of 3.82% and an optical density of 4.04, qualifying the film for use in anti-reflection chromic BM.

References:

[1] A.C. Arias, S.E. Ready, R. Lujan, W.S. Wong, K.E. Paul, A. Salleo, et al., Appl. Phys. Lett. 85 (2004) 3304.
[2] R.W. Sabnis, Displays 20 (1999) 119–129.
[3] T. Kawase, T. Shimoda, C. Newsome, H. Sirringhaus, R.H. Friend, Thin Solid Films 438–439 (2003) 279–287.
[4] H.S. Koo, P.C. Pan, T. Kawai, M. Chen, F.M. Wu, Y.T. Liu, et al., Appl. Phys. Lett. 88 (2006) 111908.
[5] R.W. Sabnis, J.W. Mayo, M.D. Stroder, E.G. Hays, A. Yanagimoto, Y. Sone, et al., Proc. Int. Display Res. Conf. 24 (1996) 0–243.
[6] A. Atkinson, Rev. Mod. Phys. 57 (1985) 437–470.
[7] T. Hasumi, T. Koseki, M. Kodate, K. Shimizu, Proc. IDRC (1996) 237–239.
[8] Y. Shima, T. Taguchi, A. Tamura, US Patent 5,925,484 (1999).
[9] H.S. Koo, M. Chen, T. Kawai, Diam. Relat. Mater. 18 (2009) 533–536.
[10] K.H. Kuo, W.Y. Chiu, K.H. Hsieh, T.M. Don, Euro. Polym. J. 45 (2009) 474–484.
[11] J.Z.Z. Zhong, A. Abileah, J.P. Hogan, N.D. Vergith, S.V. Thomsen, Proc. SPIE: Int. Soc. Opt. Eng. 3560 (1998) 49–55.
[12] Y. Hirai, H. Katoh, Proc. IDW (1995) 49–52.
[13] B. Meyer, S. Lynn, Surf. Eng. ASM Int. 5 (1994) 925.
[14] G. Irons, W. Kratochvil, M. Schroeder, C. Brock, Thermal Spray: Practical Solutions for Engineering Problems, ASM International, Ohio, USA, 1996.
[15] M. Zhang, B. Wu, G. Lin, Z. Shao, M. Hou, B. Yi, J. Power Sources 196 (2011) 3249–3254.

[16] S. Kulkarni, P. Miller, M. Wagner, J. Vac. Sci. Technol. A: Vac. Surf. Films 5 (1987) 1849–1855.
[17] A. Chen, Surf. Coat. Technol. 82 (1996) 305.
[18] G. Batis, P. Pautazopoulou, A. Routoulas, Anti-Corros. Methods Mater. 48 (2001) 674–677.
[19] S.C. Chang, Appl. Surf. Sci. 254 (2008) 2244–2249.
[20] C.D. Wagner, W.M. Riggs, L.E. Davis, J.F. Moulder, G.E. Muilenberg, Handbook of X-ray Photoelectron Spectroscopy, PerkinElmer Corporation, 1979.
[21] E. Desimoni, C. Malitesta, P.G. Zambonin, Surf. Interface Anal. 13 (1988) 173–179.
[22] I. Ikemoto, K. Ishii, S. Kinoshita, H. Kuroda, M.A.A. Franco, J.M.J. Thomas, Solid State Chem. 17 (1976) 425–430.